

Article

# Isomerization of Asp7 in Beta-Amyloid Enhances Inhibition of the $\alpha 7$ Nicotinic Receptor and Promotes Neurotoxicity

Evgeny P. Barykin <sup>1</sup>, Alexandra I. Garifulina <sup>2</sup>, Elena V. Kruykova <sup>2</sup>, Ekaterina N. Spirova <sup>2</sup>, Anastasia A. Anashkina <sup>1</sup>, Alexei A. Adzhubei <sup>1</sup>, Irina V. Shelukhina <sup>2</sup>, Igor E. Kasheverov <sup>2,3</sup>, Vladimir A. Mitkevich <sup>1</sup>, Sergey A. Kozin <sup>1</sup>, Michael Hollmann <sup>4</sup>, Victor I. Tsetlin <sup>2</sup> and Alexander A. Makarov <sup>1,\*</sup>

<sup>1</sup> Engelhardt Institute of Molecular Biology, Russian Academy of Sciences, Vavilov St. 32, 119991 Moscow, Russia

<sup>2</sup> Shemyakin-Ovchinnikov Institute of Bioorganic Chemistry, Russian Academy of Sciences, Miklukho-Maklaya Street, 16/10, 117997 Moscow, Russia

<sup>3</sup> Sechenov First Moscow State Medical University, Institute of Molecular Medicine, Trubetskaya Street 8, bld. 2, 119991 Moscow, Russia

<sup>4</sup> Department of Biochemistry I – Receptor Biochemistry, Ruhr University, 44780 Bochum, Germany

\* Correspondence: aamakarov@eimb.ru; Tel.: +7-499-135-23-11

Received: 4 June 2019; Accepted: 23 July 2019; Published: 25 July 2019



**Abstract:** Cholinergic dysfunction in Alzheimer’s disease (AD) can be mediated by the neuronal  $\alpha 7$  nicotinic acetylcholine receptor ( $\alpha 7$ nAChR). Beta-amyloid peptide (A $\beta$ ) binds to the  $\alpha 7$ nAChR, disrupting the receptor’s function and causing neurotoxicity. In vivo not only A $\beta$  but also its modified forms can drive AD pathogenesis. One of these forms, iso-A $\beta$  (containing an isomerized Asp7 residue), shows an increased neurotoxicity in vitro and stimulates amyloidogenesis *in vivo*. We suggested that such effects of iso-A $\beta$  are  $\alpha 7$ nAChR-dependent. Here, using calcium imaging and electrophysiology, we found that iso-A $\beta$  is a more potent inhibitor of the  $\alpha 7$ nAChR-mediated calcium current than unmodified A $\beta$ . However, Asp7 isomerization eliminated the ability of A $\beta$  to decrease the  $\alpha 7$ nAChR levels. These data indicate differences in the interaction of the peptides with the  $\alpha 7$ nAChR, which we demonstrated using computer modeling. Neither A $\beta$  nor iso-A $\beta$  competed with <sup>125</sup>I- $\alpha$ -bungarotoxin for binding to the orthosteric site of the receptor, suggesting the allosteric binding mode of the peptides. Further we found that increased neurotoxicity of iso-A $\beta$  was mediated by the  $\alpha 7$ nAChR. Thus, the isomerization of Asp7 enhances the inhibitory effect of A $\beta$  on the functional activity of the  $\alpha 7$ nAChR, which may be an important factor in the disruption of the cholinergic system in AD.

**Keywords:** amyloid-beta; nicotinic acetylcholine receptor; modifications; Alzheimer’s disease; neurotoxicity; calcium imaging; radioligand analysis; aspartate isomerization

## 1. Introduction

The accumulation of data on acetylcholine deficiency and the decrease of acetylcholinesterase (AChE) [1,2] in the brain of patients with Alzheimer’s disease (AD) provided the basis for the cholinergic hypothesis of AD [3]. The decrease in acetylcholine levels and AChE activity in the cortex and hippocampus observed in patients with AD may be caused by the selective death of cholinergic neurons [4]. AChE inhibitors as stimulants of the cholinergic system are one of the few drugs that alleviate AD symptoms, confirming the importance of cholinergic insufficiency in shaping the clinical picture of the disease [5]. The degeneration of cholinergic neurons may be caused by the interaction of beta-amyloid peptide (A $\beta$ ) with nicotinic acetylcholine receptors (nAChRs), which are predominantly

expressed in neurons of this type [6,7]. The two most abundant types of nAChRs in the human brain are heteromeric  $\alpha 4\beta 2$  and homomeric  $\alpha 7$ , both involved in the regulation of sleep, pain, appetite, and a number of cognitive functions [7–10]. Recent data indicate that  $\alpha 7$ nAChR is a promising target for AD therapy [11]. The  $\alpha 7$ nAChR binds to A $\beta$  with picomolar affinity, which leads to the internalization of the A $\beta$ - $\alpha 7$ nAChR complex [12] and can induce neurodegeneration [13] and plaque formation [14]. It is known that plaque formation and neurodegeneration can be triggered by structurally and chemically modified forms of A $\beta$  [15–18]. One of the most common chemical modifications of A $\beta$  is the isomerization of Asp7 residue (iso-A $\beta$ ) [19–21]. Isomerization of Asp7 is present in about 50% of A $\beta$  molecules in amyloid plaque cores [19,22]. Recent data confirm that isomerized A $\beta$  accumulates with aging and is elevated in AD [23]. There is a clear association of iso-A $\beta$  with amyloidogenesis: injections of iso-A $\beta$  aggravate amyloidosis in the brain of model mice, and an increased accumulation of iso-A $\beta$  in brain tissues of AD patients has been shown [23,24]. It can be assumed that the interaction of the  $\alpha 7$ nAChR with iso-A $\beta$  plays an important role in the disruption of cholinergic transmission and death of cholinergic neurons. In this paper, using bioinformatic approaches, calcium imaging, electrophysiology, and radioligand analysis, we studied the effects of isomerization of Asp7 in A $\beta$  on its interaction with the  $\alpha 7$ nAChR. We have shown that the isomerization of Asp7 enhances the inhibitory effect of A $\beta$  on the functional activity of the  $\alpha 7$ nAChR, which may be the reason for the increased neurotoxicity of the peptide and an important factor in the pathogenesis of AD.

## 2. Materials and Methods

### 2.1. Preparation of A $\beta$ Peptides

Synthetic Peptides: A $\beta_{42}$

[H2N]-DAEFRHDSGYEVHHQKLVFFAEDVGSNKGAIIGLMVGGVVIA-[COOH] and iso-A $\beta_{42}$ , were obtained from Biopeptide (San Diego, USA). Peptides were monomerized as described previously [25]. A fresh 5 mM solution of A $\beta$  was prepared by adding 10  $\mu$ L of 100% anhydrous dimethyl sulfoxide (DMSO) (“Sigma”) to 0.224 mg of peptide, followed by incubation for 1 h at room temperature to completely dissolve the peptide.

### 2.2. Mouse Neuroblastoma Cell Culture and Transient Transfection

Mouse neuroblastoma Neuro2a cells obtained from the Russian collection of cell cultures (Institute of Cytology, Russian Academy of Sciences, Saint Petersburg, Russia) were cultured in DMEM Dulbecco Modified Eagle Medium (DMEM) (Paneco, Moscow, Russia) supplemented with 10% FBS. They were sub-cultured the day before transfection and were plated at a density of 10,000 cells per well in a 96-well black plate. On the next day Neuro2a cells were transiently transfected with plasmids coding human  $\alpha 7$ nAChR ( $\alpha 7$ nAChR-pCEP4), a fluorescent calcium sensor Case12 (pCase12-cyto vector, Evrogen, Moscow, Russia) and chaperone NACHO (TMEM35-pCMV6-XL5, OriGene, USA) in a molar ratio of 4:1 following a lipofectamine transfection protocol (ThermoFisher Scientific, Waltham, MA, USA). Transfection with NACHO significantly increases the expression level of this receptor [26]. The transfected cells were grown at 37 °C in a CO<sub>2</sub> incubator for 48–72 h, before performing the calcium imaging assay. Cells transfected with Case12 and NACHO, but not with  $\alpha 7$ nAChR were used to calculate background.

### 2.3. Radioligand Assay

Mouse neuroblastoma Neuro2a cells transiently transfected with human  $\alpha 7$ nAChR were pre-incubated for 72 h with DMSO (final concentration 0.2%) or A $\beta_{42}$  or iso-A $\beta_{42}$  (10  $\mu$ M dissolved in DMSO) in culture medium. DMSO and the peptides were applied to cells in serum-free DMEM, and bovine serum to 10% was added 2 h later. After that,  $5 \times 10^5$  cells were incubated with 1.5 nM radioiodinated  $\alpha$ -bungarotoxin (<sup>125</sup>I- $\alpha$ Bgt) (500 Ci/mmol) in 50  $\mu$ L of DMEM (Paneco, Russia)

supplemented with protease inhibitors (PMSF, Sigma). After incubation for 30 min at room temperature, radioligand binding was stopped by filtering the incubation mixture through Whatman GF/F filters presoaked in 0.5% polyethylenimine. Then the filters were washed 3× with 4 mL cold 20 mM Tris-HCl, 0.01% BSA (pH 8.0), and bound radioactivity was measured in a Wallac 1470 Wizard Gamma Counter (PerkinElmer, Waltham, MA, USA). To determine non-specific  $^{125}\text{I}$ - $\alpha\text{Bgt}$  binding, a 200× excess of  $\alpha$ -cobratoxin [27] was added to the control samples. Specific binding was calculated as the difference between total and nonspecific binding.

#### 2.4. Competition Radioligand Assay

For a competition binding assay we used (1) the heterologously expressed acetylcholine binding protein (AChBP) from *Lymnaea stagnalis* or *Aplysia californica* or (2) the  $\alpha 7$  nAChR-transfected human cell line GH4C1. AChBP from *A. californica* and *L. stagnalis* was kindly provided by Prof. S. Luo, Key Laboratory for Marine Drugs of Haikou, Hainan University, China. The rat pituitary tumor-derived cell line GH4C1, which stably expresses human  $\alpha 7$  nAChR was received from Eli Lilly and Company, London, UK, and used immediately after defrosting without cultivation or passaging.  $^{125}\text{I}$ - $\alpha\text{Bgt}$ , which binds to AChBP and  $\alpha 7$  nAChR with 150 and 0.5 nM affinities, respectively, was used as the radioligand. AChBP and GH4C1 cells were incubated in 50  $\mu\text{L}$  of binding buffer (20 mM Tris-HCl buffer, pH 8.0, containing 1 mg/mL BSA) for 40 min with 15  $\mu\text{M}$  of amyloid peptides, followed by a 5-min incubation with 1 nM  $^{125}\text{I}$ - $\alpha\text{Bgt}$  (500 Ci/mmol). Prior to the radioactivity measurements, GH4C1 samples were filtered through glass GF/C filters (Whatman) pretreated with 0.3% polyethylenimine and washed thrice with cold 20 mM Tris-HCl buffer, pH 8.0, containing 0.1 mg/mL BSA. The AChBP samples were filtered through DE-81 filters presoaked in phosphate-buffered saline containing 0.7 mg/mL BSA and washed thrice with the same buffer. Bound radioactivity was measured as described above.

#### 2.5. Human Neuroblastoma SH-SY5Y Culture and Differentiation

Undifferentiated human neuroblastoma cells SH-SY5Y, obtained from ATCC, were cultured in DMEM/F12 medium (ThermoFisher Scientific, Waltham, MA, USA) supplemented with 10% fetal bovine serum (FBS) (PAA Laboratories GmbH, Pasching, Austria), 2.5  $\mu\text{g}/\text{mL}$  amphotericin B and 50  $\mu\text{g}/\text{mL}$  gentamicin in a  $\text{CO}_2$  incubator at 37 °C and 5%  $\text{CO}_2$  atmosphere. For differentiation, cells were sub-cultured and plated at a density of 5000–10,000 cells per well in a 96-well black plate (Corning Inc., Corning, NY, USA). *All-trans* retinoic acid (RA) (Sigma) was added the day after plating at a final concentration of 10  $\mu\text{M}$  in DMEM/F12 with 10% bovine serum. After 5 days of incubation with RA, cells were washed once with serum-free DMEM/F12 and incubated with 50 ng/mL brain-derived neurotrophic factor (Sigma) in serum-free DMEM/F12 for 3 days [28].

#### 2.6. Calcium Imaging

Calcium imaging in N2a and SH-SY5Y cells was performed according to previously published protocols [29,30]. To detect the human  $\alpha 7$  nAChR-mediated intracellular calcium rise, Case12-transfected Neuro2a cells were incubated with its positive allosteric modulator (PAM) PNU120596 [31] (10  $\mu\text{M}$ , Tocris Bioscience, Bristol, UK) for 20 min at room temperature before agonist addition. SH-SY5Y cells expressing human  $\alpha 7$  nAChRs natively were loaded with a fluorescent dye Fluo-4, AM (1.824  $\mu\text{M}$ , ThermoFisher Scientific, Waltham, MA, USA) and a water-soluble probenecid (1.25 mM, ThermoFisher Scientific, Waltham, MA, USA) for 30 min at 37 °C and then were kept for 30 min at room temperature according to the manufacturer's protocol. Then the SH-SY5Y cells were accordingly incubated with PNU120596 for 20 min before agonist addition. Transfected Neuro2a cells expressing  $\alpha 7$  nAChRs and SH-SY5Y cells expressing  $\alpha 7$  nAChRs natively were pre-incubated with  $\text{A}\beta_{42}$  or iso- $\text{A}\beta_{42}$  (10  $\mu\text{M}$ ) for 30 min at room temperature before agonist addition.  $\alpha 7$  nAChR-dependent intracellular calcium rise was induced with the highly specific  $\alpha 7$  nAChR agonist PNU282987 [32]. Pre-incubation with 15  $\mu\text{M}$  of  $\alpha$ -cobratoxin, a specific inhibitor of the  $\alpha 7$  nAChR function [27] (purified from *Naja kaouthia* venom),

for 15 min was used as a control. Measurements were performed as described previously [29,30]. Data files were analyzed using Hidex Sense software (Hidex, Turku, Finland).

### 2.7. Electrophysiology

Rat  $\alpha 7$ nAChR in the pSGEM vector were linearized using XbaI (Promega, USA). mRNAs were transcribed in vitro using the T7 mMessage mMachine (Ambion Inc., Austin, TX, USA) transcription kit. RNAs were purified by phenol:chloroform extraction and isopropanol precipitation. Stage V±VI *Xenopus laevis* oocytes were defolliculated with 2 mg/mL collagenase Type I (Life Technologies, USA) at room temperature (21–24 °C) for 2 h in Barth's solution without calcium (88.0 mM NaCl, 1.1 mM KCl, 2.4 mM NaHCO<sub>3</sub>, 0.8 mM MgSO<sub>4</sub>, 15.0 mM HEPES/NaOH, pH 7.6) for 1.5 ± 2 h at 20 °C. The oocytes were stored in Barth's solution with calcium (88.0 mM NaCl, 1.1 mM KCl, 2.4 mM NaHCO<sub>3</sub>, 0.3 mM Ca(NO<sub>3</sub>)<sub>2</sub>, 0.4 mM CaCl<sub>2</sub>, 0.8 mM MgSO<sub>4</sub>, 15.0 mM HEPES/NaOH, pH 7.6) supplemented with 63.0 µg/mL penicillin-G sodium salt, 40.0 µg/mL streptomycin sulfate, 40.0 µg/mL gentamicin.

Oocytes were selected and injected with 5 ng cRNA of rat  $\alpha 7$ nAChR in a total injection volume of 15 nL. After the injection, the oocytes were incubated at 18 °C in ND96 buffer or in Barth's solution with calcium for 48 ± 120 h. Electrophysiological recordings were made using a Turbo TEC-03X amplifier (Npi electronic, Germany) and Patch master software (HEKA, Germany), at a holding potential of −60 mV. Oocytes were placed in a small recording chamber with a working volume of 50 µL, and 50–100 µL of agonist (acetylcholine) solution in ND96 electrophysiological buffer or Ba<sup>2+</sup> Ringer's solution (115.0 mM NaCl, 2.5 mM KCl, 1.8 mM BaCl<sub>2</sub>, 10.0 mM HEPES/NaOH, pH 7.2) were applied to an oocyte. Oocytes expressing rat  $\alpha 7$ nAChR were pre-incubated with A $\beta$ <sub>42</sub> or iso-A $\beta$ <sub>42</sub> (10 µM) for 3 min followed by its co-application with acetylcholine (3–1000 µM). To allow receptor recovery from desensitization, the oocytes were superfused for 5 ± 10 min with buffer (1 mL/min) between the ligand applications.

### 2.8. Modelling of A $\beta$ : $\alpha 7$ nAChR and Iso-A $\beta$ : $\alpha 7$ nAChR Interaction

Modelling of the A $\beta$ <sub>42</sub> three-dimensional structure has been performed using templates selected from a survey of A $\beta$  structures in the PDB database which we carried out earlier [33]. We have also utilized results of ab initio modeling with the Bhageerath server [34]. The subsequent expert modeling and energy minimization was followed by computation of molecular dynamics (MD) trajectories for the obtained A $\beta$ <sub>42</sub> structure, yielding the final model structure [35].

The three-dimensional structure of the iso-A $\beta$ <sub>42</sub> has been modeled applying a similar MD technique. Prior to this, modelling of the isomerized D7 residue in the A $\beta$ <sub>42</sub> structure has been performed. The  $\alpha 7$ nAChR extracellular domain structure has been modeled by the Swiss Model server using the structures of  $\alpha 7$ nAChR-AChBP chimeras 5AFJ and 3SQ6 from the Protein Data Bank as the templates.

Modeling of interaction was carried out by global docking using the QASDOM meta-server (<http://qasdom.eimb.ru/>) developed by us [36]. Sets of A $\beta$ <sub>42</sub> and iso-A $\beta$ <sub>42</sub> models interacting with the extracellular domain of  $\alpha 7$ nAChR were obtained by global docking using Gramm-x, ClusPro, SwarmDock, and Zdockweb-servers.

### 2.9. Neurotoxicity Measurements

Human neuroblastoma cells SH-SY5Y were differentiated as described above in 96-well plates. Differentiated cells were incubated with 10 µM of A $\beta$ <sub>42</sub> or iso-A $\beta$ <sub>42</sub> for 72 h in serum-free media in the presence of 20 ng/mL BDNF. After the incubation, cells were washed with PBS and stained with either 1 µM EthD-1 (Thermo Scientific) for 30 min at 37 °C or WST reagent (Sigma), diluted in culture media 1:10 for 2 h at 37 °C. EthD fluorescence and absorbance of WST was measured with a Spark microplate reader (Tecan).

### 2.10. Statistical Methods Used for Data Analysis

Data are presented as means of at least three independent experiments  $\pm$  SD or SE. The comparison of data groups in toxicity tests and in radioligand assay was performed using one-way ANOVA with post-hoc testing (using unpaired samples Student's *t*-test with Bonferroni correction); after a Bonferroni correction a *p* value  $< 0.016$  was considered as statistically significant. Statistical analysis was performed using STATISTICA 8.0 (StatSoft Inc., Tulsa, OK, USA) and OriginPro 9.0 software (OriginLab, Northampton, MA, USA).

## 3. Results

### 3.1. Effects of $A\beta_{42}$ and Iso- $A\beta_{42}$ on Functional Activity of $\alpha 7nAChR$ in N2a and SH-SY5Y Cells and in *Xenopus Laevis* Oocytes

To study the effects of  $A\beta_{42}$  and iso- $A\beta_{42}$  on the  $\alpha 7nAChR$ , we used two cell lines expressing  $\alpha 7nAChR$ . The first one, the human neuroblastoma cell line SH-SY5Y, expresses  $\alpha 7nAChR$  endogenously. To achieve neuron-like expression patterns and morphology, it was differentiated as described above. The second line, mouse neuroblastoma N2a, was co-transfected with  $\alpha 7nAChR$  and the chaperone NACHO. The efficiency of the transfection in N2a cells was confirmed with fluorescent  $\alpha$ -bungarotoxin staining (Figure S1) as described previously [30]. Receptor function studies were performed with the calcium imaging technique. We observed a robust response of both cell lines to  $\alpha 7nAChR$  stimulation and the determined half maximal effective concentration (EC50) for the agonist PNU282987 was close to published values (Figure S2A) [36]. The kinetics and the amplitude of the response did not depend on the calcium sensor used (fluo-4 in SH-SY5Y or Case12 in N2a) (Figure S2B), which correlates with the previously published data, where we have shown the equivalence of fluo-4 and Case12 in N2a for analysis of both the  $\alpha 7nAChR$  and the muscle-type nAChR functional activity [30].

Pre-incubation with  $A\beta_{42}$  or iso- $A\beta_{42}$  for 30 min significantly suppressed the intracellular calcium rise in SH-SY5Y and  $\alpha 7nAChR$ -transfected N2a cells, induced by PNU282987 (Figure 1A,B). We did not observe any response in  $\alpha 7nAChR$ -untransfected N2a cells, and the application of  $\alpha$ -cobratoxin completely suppressed the calcium rise in both SH-SY5Y and  $\alpha 7nAChR$ -transfected N2a cells, indicating that the observed response was mediated by the  $\alpha 7nAChR$  [27]. The effects of  $A\beta_{42}$  and iso- $A\beta_{42}$  were different in both the intensity of the inhibition and in their inhibition pattern. In N2a cells, the  $A\beta_{42}$  peptide inhibited the receptor response by 30% at the maximum concentration of PNU282987, whereas for iso- $A\beta_{42}$  the degree of inhibition reached 60%. In addition, the inhibitory effect of the peptides differed sharply depending on the concentration of PNU282987. Thus, inhibition of the  $\alpha 7nAChR$  by the  $A\beta_{42}$  peptide was not observed at 30 or 60 nM of PNU282987, whereas iso- $A\beta_{42}$  inhibited the receptor response by 90% at these concentrations of PNU282987, as compared with the control (Figure 1A). In the SH-SY5Y cells, the inhibition of the  $\alpha 7nAChR$  by the  $A\beta_{42}$  and iso- $A\beta_{42}$  peptides did not differ at the maximum concentration of PNU282987; however, at low concentrations of the agonist, we observed differences in the action of the peptides similar to those obtained in the N2a cells (Figure 1B). In both cell lines, the incubation with iso- $A\beta_{42}$  increased the EC50 of the  $\alpha 7nAChR$  for PNU282987, while  $A\beta_{42}$  had virtually no effect (in N2a cells) or even decreased (in SH-SY5Y cells) the EC50 (Table 1).

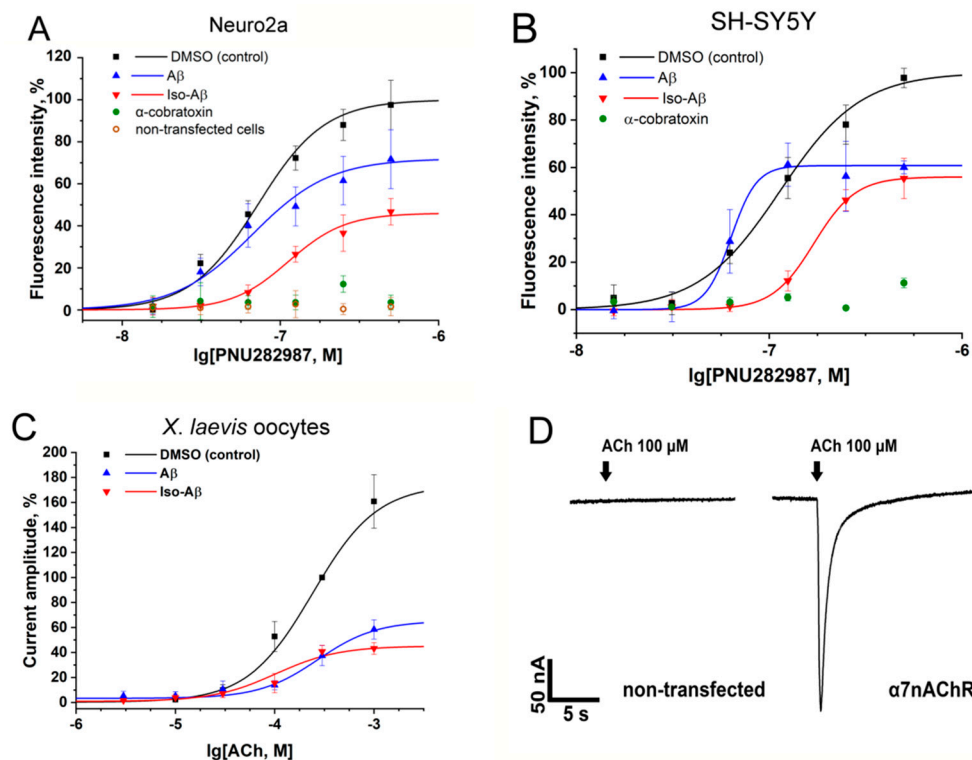


**Figure 1.** Effects of Aβ<sub>42</sub> and iso-Aβ<sub>42</sub> on the intracellular Ca<sup>2+</sup> and Ba<sup>2+</sup> rise mediated by the α7nAChR. Dose-dependent Ca<sup>2+</sup> response to PNU282987 stimulation (A) in α7nAChR-transfected or in non-transfected N2a and (B) in differentiated SH-SY5Y cells pre-incubated with 10 μM of Aβ<sub>42</sub> or iso-Aβ<sub>42</sub> for 30 min or with 15 μM of α-cobratoxin for 15 min. (C) Dose-dependent Ba<sup>2+</sup> response in the α7nAChR-transfected *Xenopus laevis* oocytes to acetylcholine (ACh) stimulation after 3 min pre-incubation with 10 μM of Aβ<sub>42</sub> or iso-Aβ<sub>42</sub>. (D) Electrophysiological recordings of α7nAChR currents in native (uninjected) and α7nAChR cRNA-injected oocytes. Currents were obtained in response to 100 μM ACh application (arrows). Vertical bar represents current scale (50 nA). Data are presented as the mean ± SEM of at least three independent experiments.

**Table 1.** The half maximal effective concentration (EC<sub>50</sub>) of PNU282987 inducing the α7nAChR-mediated intracellular calcium rise in N2a and SH-SY5Y neuroblastoma cell lines, treated with Aβ<sub>42</sub> or iso-Aβ<sub>42</sub>. Data are presented as the mean of at least three independent experiments ± SEM.

Cell Line	Treatment	EC50 Value, nM
N2a	Control	71.9 ± 8.4
	Aβ <sub>42</sub>	66.8 ± 8.6
	iso-Aβ <sub>42</sub>	112.6 ± 4.3
SH-SY5Y	Control	114 ± 7.0
	Aβ <sub>42</sub>	63.4 ± 2.3
	iso-Aβ <sub>42</sub>	171 ± 3.3

The effects of Aβ<sub>42</sub> and iso-Aβ<sub>42</sub> were also analyzed by two-electrode voltage clamp in *X. laevis* frog oocytes expressing the α7nAChR. The application of acetylcholine to oocytes pre-incubated with the amyloid peptides for 3 min showed an inhibition of the currents by both Aβ<sub>42</sub> and iso-Aβ<sub>42</sub> (Figure 1C). The effects of the peptides observed in the oocytes were almost identical, with the exception of the slightly larger (by 10%) inhibitory effect of iso-Aβ<sub>42</sub> at the maximum acetylcholine concentration used (1 mM). The inhibitory effect of the amyloid peptides on the α7nAChR in *X. laevis* oocytes, as in the N2a cells, increased along with the increasing concentration of the agonist. The observed responses

in the oocytes were characteristic for the  $\alpha 7$ nAChR, and no ACh-induced currents were detected in the  $\alpha 7$ nAChR cRNA-uninjected oocytes (Figure 1D).

### 3.2. $A\beta_{42}$ and Iso- $A\beta_{42}$ Do not Compete with $\alpha$ -Bungarotoxin for Binding to the $\alpha 7$ nAChR or to Acetylcholine-Binding Proteins (AChBPs)

The differences in the affinity of the amyloid peptides for the  $\alpha 7$ nAChR were studied with a competitive radioligand assay using radioiodinated  $\alpha$ -bungarotoxin ( $^{125}\text{I}$ - $\alpha$ Bgt). The ability of  $A\beta_{42}$  and iso- $A\beta_{42}$  at a concentration of 15  $\mu\text{M}$  to inhibit  $^{125}\text{I}$ - $\alpha$ Bgt binding was studied on the  $\alpha 7$ nAChR expressed in GH4C1 cells and on purified recombinant acetylcholine-binding proteins (AChBPs) from *Aplysia californica* and *Lymnaea stagnalis*. Neither  $A\beta_{42}$  nor iso- $A\beta_{42}$  inhibited the binding of  $^{125}\text{I}$ - $\alpha$ Bgt to the AChBPs (Figure S3A) after 40 min of pre-incubation. In addition, no significant inhibition by the amyloid peptides of  $^{125}\text{I}$ - $\alpha$ Bgt binding to the  $\alpha 7$ nAChR expressed by the GH4C1 cells was detected (Figure S3B).

### 3.3. The $A\beta_{42}$ -Induced Reduction of $\alpha 7$ nAChR Representation is Neutralized by the Isomerization of Asp7

Since we observed no inhibition of the binding of  $^{125}\text{I}$ - $\alpha$ Bgt to the  $\alpha 7$ nAChR or AChBPs after 40 min of pre-incubation with the amyloid peptides, we decided to test how a prolonged incubation with  $A\beta_{42}$  or iso- $A\beta_{42}$  would affect the level of the  $\alpha 7$ nAChR. It has previously been established that prolonged incubation with  $A\beta_{42}$  results in a decrease in the  $\alpha 7$ nAChR expression in PC12 neuroblastoma cells [37]. To test the effect of the peptides on the receptor levels, we used N2a neuroblastoma cells, which transiently express the  $\alpha 7$ nAChR. The incubation of the N2a cells with  $A\beta_{42}$  for 72 h resulted in a 35% decrease in the specific binding of  $^{125}\text{I}$ - $\alpha$ Bgt to the  $\alpha 7$ nAChR (Figure 2), indicating a decrease in the  $\alpha 7$ nAChR levels in N2a cells. The incubation with iso- $A\beta_{42}$  did not affect the amount of  $^{125}\text{I}$ - $\alpha$ Bgt bound to the cells.

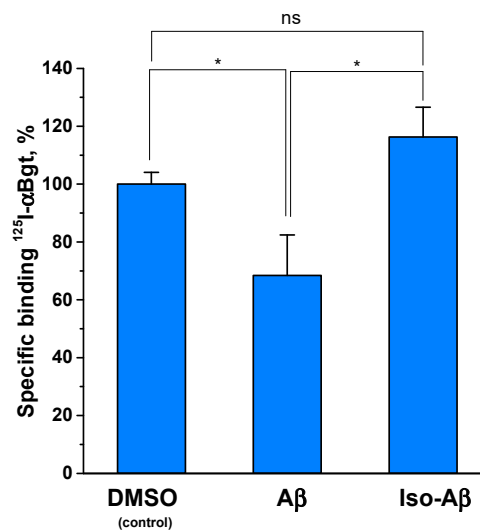


**Figure 2.** Specific binding of  $^{125}\text{I}$ - $\alpha$ Bgt to Neuro2a cells transiently transfected with human  $\alpha 7$ nAChR. The cells were pre-incubated for 72 h with either 0.4% DMSO (control) or 10  $\mu\text{M}$  of  $A\beta_{42}$  or iso- $A\beta_{42}$  dissolved in DMSO. Specific binding in the control is set to 100%. Data are presented as the mean  $\pm$  SEM of two independent experiments with at least five replicates for each point. \*  $p < 0.05$ , ns = non-significant.

### 3.4. Comparison of the Toxicity of $A\beta_{42}$ and Iso- $A\beta_{42}$ toward SH-SY5Y Cells

The effects of  $A\beta_{42}$  and iso- $A\beta_{42}$  on the  $\alpha 7$ nAChR differed not only for the short-term but also for the long-term incubation of cells with the peptides. It is known that the  $\alpha 7$ nAChR can mediate the toxic effect of  $A\beta_{42}$  on neuronal cells [38], so we tested how the isomerization of Asp7 changes the  $\alpha 7$ nAChR-mediated cytotoxicity of  $A\beta_{42}$ . To this end, we examined the neurotoxic effects of  $A\beta_{42}$  and iso- $A\beta_{42}$  on differentiated SH-SY5Y neuroblastoma cells in the presence and absence of the

selective  $\alpha 7nAChR$  inhibitor  $\alpha$ -bungarotoxin ( $\alpha$ Bgt). The incubation of SH-SY5Y cells with  $A\beta_{42}$  for 72 h resulted in a 25% increase in necrotic cells (Figure 3A) and a 5–7% decrease in cell viability (Figure 3B). The iso- $A\beta_{42}$  showed a higher neurotoxicity with a 60% increase in the number of necrotic cells, and the cell viability decreased by 25%. The toxic effect of  $\alpha$ Bgt at a concentration of 50 nM was similar in magnitude to the effect of iso- $A\beta_{42}$ . The co-application of  $A\beta_{42}$  with  $\alpha$ Bgt caused a toxic effect similar to that of iso- $A\beta_{42}$  (Figure 3B, in the middle), while the simultaneous addition of iso- $A\beta_{42}$  and  $\alpha$ Bgt did not change the toxicity (Figure 3A,B, righthand columns). The higher neurotoxicity of iso- $A\beta_{42}$  compared to that of  $A\beta_{42}$  was not due to its enhanced aggregation or differences in oligomeric composition (Figure S4), as we demonstrated by the electrophoretic analysis of covalently linked low-molecular weight oligomers obtained by photo-induced cross-linking (Supplementary Methods) [39].

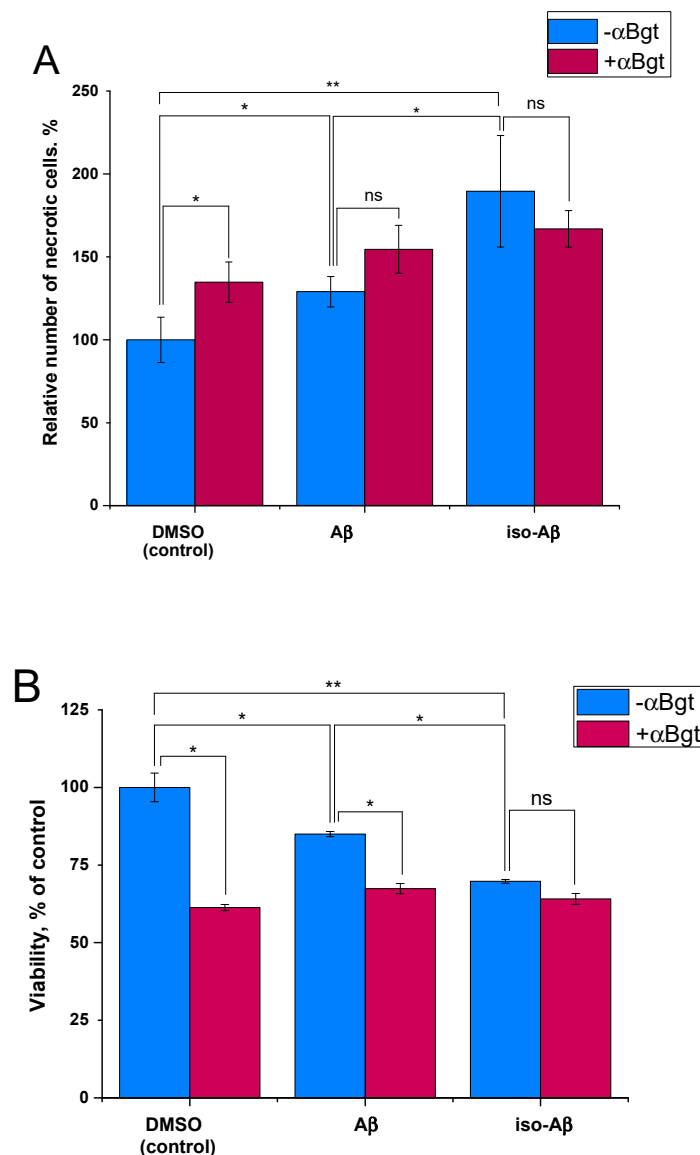


**Figure 3.** Neurotoxic effects of  $A\beta_{42}$  and iso- $A\beta_{42}$  on differentiated SH-SY5Y cells were measured after 72 h of incubation with 10  $\mu$ M of peptides in the presence or absence of  $\alpha$ -bungarotoxin ( $\alpha$ Bgt) (50 nM). **(A)** Relative number of necrotic cells—represented by normalized Ethidium dimer (EthD-1) fluorescence. **(B)** Viability of cells in relation to the control—measured with the WST test. Data are presented as the mean  $\pm$  SD of two independent experiments with at least five replicates for each point. \*  $p < 0.05$ , \*\*  $p < 0.01$ , ns = non-significant.

### 3.5. Molecular Modeling of the Binding Sites for Iso-A $\beta_{42}$ and A $\beta_{42}$ in the $\alpha 7nAChR$

To obtain additional data on how Asp7 isomerization affects the interaction of A $\beta_{42}$  with the  $\alpha 7nAChR$ , we constructed the models of peptide–receptor complexes using molecular modeling. Using the A $\beta_{42}$  structure as the initial model [33], the iso-A $\beta_{42}$  model was created. The modeling showed that the isomerization of Asp7 significantly changed the structure of the peptide (Figure 4A). The sets of A $\beta_{42}$  and iso-A $\beta_{42}$  complexes with the  $\alpha 7nAChR$  extracellular domain obtained on Gramm-x, ClusPro, SwarmDock, and Zdock servers were analyzed using the QASDOM meta-server. The modeling of the receptor–peptide complexes indicated the presence of common binding sites for A $\beta_{42}$  and iso-A $\beta_{42}$  (inside the receptor channel), as well as different binding sites on the outer surface of the receptor (Figure 4B). An analysis of the probability of the interaction of the peptides with different  $\alpha 7nAChR$  amino acid residues (Figure S5) showed that the predicted peptide binding sites overlap with the acetylcholine binding site and the known allosteric binding sites [40,41]. For both A $\beta_{42}$  and iso-A $\beta_{42}$ , bindings to Loop E and Loop F of the agonist-binding pocket were predicted. By contrast, a strong binding in the Loop C region was observed for A $\beta_{42}$  but was completely absent for iso-A $\beta_{42}$ . For both peptides we predicted binding in the regions of 6–15 and 64–72, the amino acid residues of which participate in the formation of the “top pocket” allosteric site, and in the region of 97–103, which forms part of the “vestibule pocket” allosteric site [41], with the binding of A $\beta_{42}$  in the “top pocket” being much stronger (Figure S5). On the other hand, binding to the L38 residue, which is part of another allosteric site, the “agonist subpocket”, was predicted for iso-A $\beta_{42}$  only [41]. For both peptides, an interaction with the Trp55 residue, which is critical for the rapid desensitization of the receptor [42], was predicted. In the resulting models, both A $\beta_{42}$  and iso-A $\beta_{42}$  demonstrated an interaction in the region of residues 55–61. It has previously been shown that a peptide corresponding to these residues is able to destroy the A $\beta$  complex with the receptor [43]. Another peptide with similar properties corresponds to residues 146–155, and in this area we predicted binding for A $\beta_{42}$  but not for iso-A $\beta_{42}$ . In areas not related to known binding sites, with the exception of the area of 129–142, interaction was not observed. In the area of 129–142, which corresponds to the distal (upper) part of the receptor (Figure 4B), binding was predicted only for iso-A $\beta_{42}$ .

Amino acid residue-wise analysis of A $\beta_{42}$  and iso-A $\beta_{42}$  interaction with the receptor suggested a possible basis for the differences in the inhibitory effects of the peptides (Figure S6). Compared to A $\beta_{42}$ , binding of iso-A $\beta_{42}$  to the  $\alpha 7nAChR$  is significantly reduced for the residues 7–10 of the peptide, probably reflecting a sharp turn (Figure 4A) occurring in the peptide secondary structure due to the Asp7 isomerization. The hydrophobic C-terminus of iso-A $\beta_{42}$ , comprising residues 27 till 40, forms an inward loop, which leads to weaker binding of this region to the  $\alpha 7nAChR$  than in A $\beta_{42}$ . On the contrary, in iso-A $\beta_{42}$  stronger binding to the  $\alpha 7nAChR$  was predicted around the residues 11–16 and for the residue Phe20.

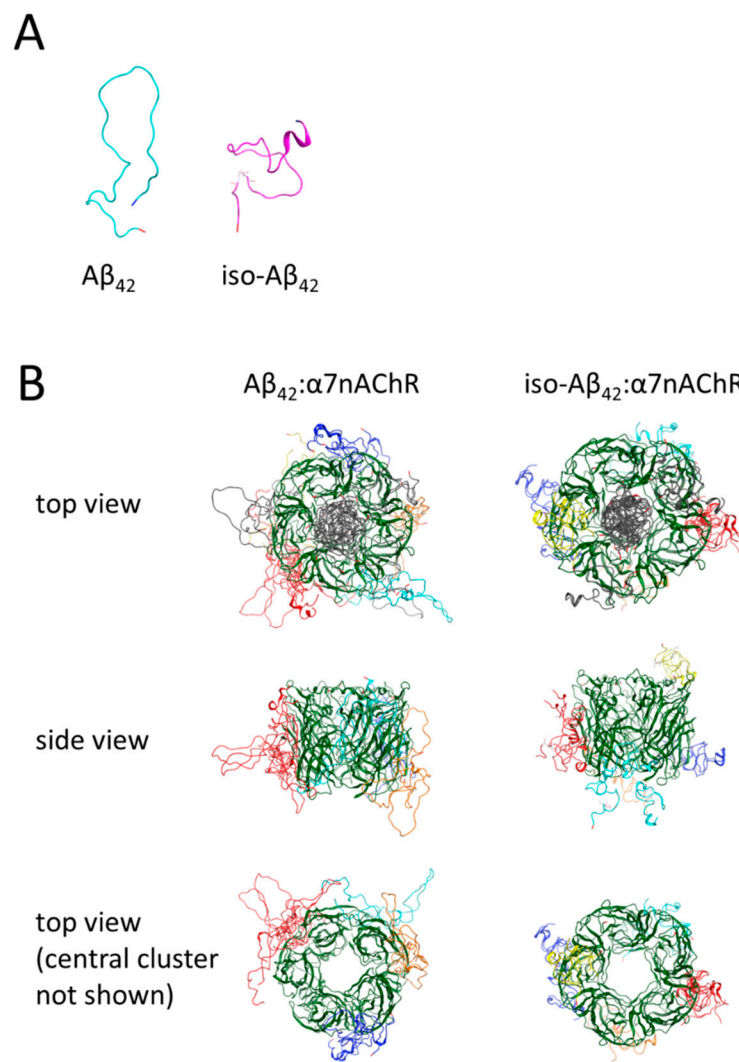


**Figure 4.** (A) Models of  $A\beta_{42}$  and iso- $A\beta_{42}$  in solution. (B) Models of the  $\alpha 7nAChR$  complexes with the amyloid peptides.

#### 4. Discussion

The disruption of cholinergic transmission in AD was one of the first detected phenomena that determine the clinical picture of the disease [44]. Loss of nicotinic receptors in the brain tissues of patients has been observed with both a reduction in the number of ligand binding sites and a reduction of the levels of the receptor subunits [45]. The  $\alpha 7nAChR$  is well-presented in brain tissue and is an important component of the cholinergic system involved in memory formation [14]. It is known that the  $A\beta_{42}$  peptide is able to bind to the  $\alpha 7nAChR$  with high affinity [13], which leads to the inhibition of the receptor [46], neuron death [13], and may precede the formation of plaques [14].

In the sporadic form of AD, neurodegeneration and amyloidogenesis can be induced by modified forms of  $A\beta$  [15–18]. One of these forms is iso- $A\beta$ , which has a stronger neurotoxic and amyloidogenic effect than  $A\beta$  [24,47].

We compared the inhibitory properties of iso- $A\beta_{42}$  and  $A\beta_{42}$  toward the  $\alpha 7nAChR$ . For the measurements, we used the  $\alpha 7nAChR$  transiently expressed in N2a cells [30] and in *X. laevis* oocytes [48], or endogenously expressed in differentiated SH-SY5Y cells [49,50]. Previously, we utilized the  $\alpha 7nAChR$ -transfected N2a cells and  $\alpha 7nAChR$  cRNA-injected *X. laevis* oocytes to analyze the interaction of the receptor with various natural [51] and synthetic [52] low-molecular compounds, neurotoxic peptides and proteins [53], as well as with human toxin-like three-finger proteins [48,54]. Both  $A\beta_{42}$

and iso-A $\beta_{42}$  inhibited intracellular calcium rise caused by  $\alpha 7$ nAChR activation in differentiated SH-SY5Y cells or in N2a cells (Figure 1). However, iso-A $\beta_{42}$  showed a greater suppression of the receptor-induced increase in the concentration of intracellular Ca<sup>2+</sup> (Figure 1A) and, unlike A $\beta_{42}$ , the effect of iso-A $\beta_{42}$  did not disappear with a decrease in the concentration of the agonist (Figure 1A,B). Thus, the isomerization of Asp7 leads to an increase in the intensity of inhibition and a change in the nature of the inhibitory effect of A $\beta_{42}$  on the  $\alpha 7$ nAChR. To confirm the interaction between the  $\alpha 7$ nAChR and the peptides, we measured the effects of iso-A $\beta_{42}$  and A $\beta_{42}$  in  $\alpha 7$ nAChR-transfected *X. laevis* oocytes. The oocytes represent a pure system without factors affecting the interaction, such as the presence of the other nicotinic receptors or the positive allosteric modulator PNU120596. The use of PNU120596 in calcium imaging is inevitable since it amplifies agonist-induced  $\alpha 7$ nAChRs responses to the detectable level. PNU120596 increases the probability of transient  $\alpha 7$ nAChR activation by agonists, and also destabilizes a ligand-bound non-conducting “desensitized” state of the receptor [55–57]. In oocytes, both iso-A $\beta_{42}$  and A $\beta_{42}$  exhibited an inhibitory effect on the  $\alpha 7$ nAChR, however, these effects hardly differed (Figure 1C). Such similarity can be attributed to the absence of secondary effects in oocytes due to  $\alpha 7$ nAChR internalization, alteration of membrane potential, or induced by Ca<sup>2+</sup> entry. The electrophysiology was performed in the absence of Ca<sup>2+</sup> in Ba<sup>2+</sup>-containing buffer, which also prevents current inactivation and receptor desensitization due to acute Ca<sup>2+</sup> rise [58–60]. In contrast to previously published data [13,61], our results show that both A $\beta_{42}$  and iso-A $\beta_{42}$  are noncompetitive  $\alpha 7$ nAChR inhibitors that bind at the allosteric site. Both in experiments on cell lines and in *X. laevis* oocytes, incubation with peptides reduced the maximum response of the receptor, which became even more pronounced with increasing concentrations of the agonist, indicating a non-competitive inhibition. In addition, we observed an increase in the inhibitory effect of peptides with an increase in the concentration of the agonist, which is also a property of allosteric inhibitors [48,62]. The allosteric nature of the binding was confirmed by the lack of competition between  $\alpha$ Bgt, the orthosteric inhibitor of  $\alpha 7$ nAChR, and the amyloid peptides both in binding to an AChBP and to the  $\alpha 7$ nAChR in GH4C1 cells (Figure S3).

Despite the lack of competition between the amyloid peptides and  $\alpha$ Bgt during a 40 min incubation, the incubation of N2a cells with A $\beta_{42}$  for 72 h caused a 30% decrease in  $\alpha$ Bgt binding to the cells (Figure 2). Since A $\beta$  does not compete with  $\alpha$ Bgt, this effect was due to a 30% decrease in  $\alpha 7$ nAChR levels in the N2a cells. According to the literature, the formation of the A $\beta$ – $\alpha 7$ nAChR complex leads to the endocytosis of the peptide–receptor complex [63] and a decrease in the level of the  $\alpha 7$ nAChR [37]. Taking into account the stronger inhibitory effect of iso-A $\beta_{42}$  on the receptor, we expected to see the same or more pronounced effect of this peptide on the expression of the  $\alpha 7$ nAChR. However, iso-A $\beta_{42}$  had no effect on the level of the receptor in N2a cells (Figure 2). It is possible that the actions of the intact and modified peptides on the receptor not only differ in the strength of the inhibition but suggests qualitatively different mechanisms of interaction with the receptor. The differences in the action of A $\beta_{42}$  and iso-A $\beta_{42}$  on the  $\alpha 7$ nAChR level may also be related to the effect on the assembly of receptors inside the cell, as has been shown for other nAChR allosteric modulators of the human Ly6 family [64,65].

The molecular modeling data agree with the qualitative differences in the interaction of intact and modified peptides with the receptor. According to the simulation results, the isomerization of the Asp7 residue introduces significant changes into the spatial structure of A $\beta_{42}$  (Figure 4A). These structural changes are reflected in different binding modes of A $\beta_{42}$  and iso-A $\beta_{42}$  to the receptor (Figure S6). In A $\beta_{42}$ , the residues surrounding Asp7 and the C-terminal hydrophobic domain are more involved in binding to the receptor, whereas in iso-A $\beta_{42}$  interaction with the  $\alpha 7$ nAChR is strongly mediated by the residues 11–16, compared to the unmodified A $\beta_{42}$ . The model structures of the iso-A $\beta_{42}$  and A $\beta_{42}$  complexes with the  $\alpha 7$ nAChR are quite similar to each other (Figure 4B), however, the binding of the peptides was different in certain areas. A weaker interaction was predicted for iso-A $\beta_{42}$  with the top-pocket allosteric site (Figure S5) and a stronger interaction with the region of 129–142 of the receptor, the function of which is not known [42]. The prediction of the allosteric nature of the interaction

*in silico* is consistent with the data obtained experimentally *in vitro*, namely with the inhibitory pattern of the amyloid peptides. The differences in the interaction of the peptides with the  $\alpha 7$ nAChR are also consistent with the differences in the action of the peptides on the intracellular calcium rise mediated by the  $\alpha 7$ nAChR and with their effects on the expression of the receptor.

It is known that the  $\alpha 7$ nAChR can mediate the neurotoxicity of A $\beta$ . The  $\alpha 7$ nAChR modulates fundamental pathways involved in cell survival such as JAK2-STAT3 and the reported binding of  $\beta$ -amyloid to the  $\alpha 7$ nAChR can effectively decouple the receptors from key pro-survival pathways [14]. A $\beta$  inhibits the response of  $\alpha 7$ nAChR-containing hippocampal neurons [46], and the neurotoxicity of A $\beta$  decreases with the presence of receptor agonists [38,66,67].  $\alpha 7$ nAChR-mediated Ca<sup>2+</sup> influx directly promotes cell survival [68–70], and inhibition of this Ca<sup>2+</sup> current by A $\beta$  may contribute to neurotoxicity of the peptide.

We decided to test whether the increased ability of iso-A $\beta_{42}$  peptide to inhibit the  $\alpha 7$ nAChR-mediated Ca<sup>2+</sup> influx affects its neurotoxic properties. Iso-A $\beta_{42}$  was found to have an increased toxicity for  $\alpha 7$ nAChR-expressing differentiated SH-SY5Y neuroblastoma cells, which is consistent with the data previously obtained on undifferentiated SH-SY5Y cells or on immortalized H-TERT neurons [47,71]. Importantly, lower concentrations of A $\beta$  neither reproduce toxic effects of such magnitude nor the A $\beta$ -induced loss of nicotinic receptors. These findings suggest that iso-A $\beta_{42}$  toxicity is due to an inhibition of the  $\alpha 7$ nAChR: the toxic effect of iso-A $\beta_{42}$  is similar in magnitude to that of  $\alpha$ Bgt, and their co-application does not lead to an increase in cell death (Figure 3). Apparently, both  $\alpha$ Bgt and iso-A $\beta_{42}$  induce the maximal  $\alpha 7$ nAChR-mediated level of cell death under these conditions, therefore their effects are not additive. Thus, the increased toxicity of iso-A $\beta_{42}$  may be due to a stronger inhibition of the  $\alpha 7$ nAChR by this peptide. Some studies report that A $\beta$  toxicity can be mediated by the intracellular Ca<sup>2+</sup> rise [72–74], however, our data supports the protective role of Ca<sup>2+</sup> entry, at least through the  $\alpha 7$ nAChR.

In general, the analysis of the interactions of modified forms of A $\beta$  with the  $\alpha 7$ nAChR may be crucial for the development of new therapies for AD. In this study, we showed that Asp7 isomerization in A $\beta$  enhances the inhibitory effect of A $\beta$  on the  $\alpha 7$ nAChR and leads to a more pronounced neurotoxic effect of the peptide. The  $\alpha 7$ nAChR is widely distributed in the CNS and in the cells of the immune system, while iso-A $\beta$  is one of the most common modifications of A $\beta$  in patients with AD. Thus, to effectively treat AD through the restoration of the  $\alpha 7$ nAChR function, it may be necessary to target an isomerized form of A $\beta$ , which differs from A $\beta$  in its interaction with the receptor.

**Supplementary Materials:** The following are available online at <http://www.mdpi.com/2073-4409/8/8/771/s1>, Supplementary Methods: Fluorescent  $\alpha$ -bungarotoxin binding assay; Photo-induced cross-linking of amyloid peptides; Figure S1: Cytochemical staining of (A, B) N2a cells transfected with plasmids coding human  $\alpha 7$ nAChR, chaperone NACHO and calcium sensor Case12 and (C, D) of non-transfected cells with 50 nM Alexa Fluor 555- $\alpha$ -bungarotoxin (red). Scale bar, 50  $\mu$ m. Figure S2: (A) Dose-dependent response of  $\alpha 7$ nAChR to PNU-282897 stimulation in Neuro2a and differentiated SH-SY5Y (SH-SY5Y diff) cell lines, (B) Kinetics of the  $\alpha 7$ nAChR-mediated intracellular single-cell Ca<sup>2+</sup> response to PNU282987 (500 nM) stimulation in Neuro2a cell expressing the fluorescent Ca<sup>2+</sup> sensor Case12 and in SH-SY5Y cell, loaded with a fluorescent dye Fluo-4. a.u. – arbitrary units; Figure S3. Analysis of A $\beta_{42}$  and iso-A $\beta_{42}$  competition with radioiodinated  $\alpha$ -bungarotoxin (125I- $\alpha$ Bgt) for binding to (A) the acetylcholine-binding protein (AChBP) from *L. stagnalis* (left panel) or *A. californica* (right panel) and (B) to the  $\alpha 7$ nAChR of GH4C1 cells; Figure S4: The relative amount of A $\beta_{42}$  and iso-A $\beta_{42}$  peptides in various aggregation states, determined by photo-induced chemical cross-linking; Figure S5: The probability of binding of A $\beta$  (upper part) and iso-A $\beta$  (lower part) peptides to amino acid residues of extracellular part of  $\alpha 7$ nAChR; Figure S6: The probability of amino acid residues binding of A $\beta_{42}$  (upper panel) and iso-A $\beta_{42}$  (lower panel) peptides to extracellular part of the  $\alpha 7$ nAChR.

**Author Contributions:** Conceptualization, I.V.S., S.A.K. and V.I.T.; Funding acquisition, A.A.M.; Investigation, E.P.B., A.I.G., E.V.K., E.N.S., A.A.A. (Anastasia A. Anashkina) and A.A.A. (Alexei A. Adzhubei); Methodology, M.H. and V.I.T.; Resources, I.E.K., M.H., V.I.T. and A.A.M.; Software, A.A.A. (Anastasia A. Anashkina) and A.A.A. (Alexei A. Adzhubei); Visualization, A.A.A. (Alexei A. Adzhubei); Writing—original draft, E.P.B., A.I.G., E.V.K., A.A.A. (Anastasia A. Anashkina), A.A.A. (Alexei A. Adzhubei) and V.A.M.; Writing—review & editing, I.V.S., I.E.K., S.A.K., M.H., V.I.T. and A.A.M.

**Funding:** This research was funded by the RUSSIAN SCIENCE FOUNDATION, grant number 19-74-30007.

**Conflicts of Interest:** The authors declare no conflict of interest. The funders had no role in the design of the study; in the collection, analyses, or interpretation of data; in the writing of the manuscript, or in the decision to publish the results.

## References

1. Whitehouse, P.J.; Martino, A.M.; Marcus, K.A.; Zweig, R.M.; Singer, H.S.; Price, D.L.; Kellar, K.J. Reductions in Acetylcholine and Nicotine Binding in Several Degenerative Diseases. *Arch. Neurol.* **1988**, *45*, 722–724. [[CrossRef](#)] [[PubMed](#)]
2. Herholz, K. Acetylcholine esterase activity in mild cognitive impairment and Alzheimer's disease. *Eur. J. Nucl. Med. Mol. Imaging* **2008**, *35*, 25–29. [[CrossRef](#)] [[PubMed](#)]
3. Appel, S.H. A unifying hypothesis for the cause of amyotrophic lateral sclerosis, parkinsonism, and alzheimer disease. *Ann. Neurol.* **1981**, *10*, 499–505. [[CrossRef](#)] [[PubMed](#)]
4. Wenk, G.L. Neuropathologic changes in Alzheimer's disease. *J. Clin. Psychiatry* **2003**, *64 Suppl 9*, 7–10.
5. Stahl, S.M. The New Cholinesterase Inhibitors for Alzheimer's Disease, Part 2: Illustrating Their Mechanisms of Action: (Brainstorms). *J. Clin. Psychiatry* **2000**, *61*, 813–814. [[CrossRef](#)] [[PubMed](#)]
6. Albuquerque, E.X.; Pereira, E.F.R.; Alkondon, M.; Rogers, S.W. Mammalian Nicotinic Acetylcholine Receptors: From Structure to Function. *Physiol. Rev.* **2009**, *89*, 73–120. [[CrossRef](#)] [[PubMed](#)]
7. Gotti, C.; Clementi, F. Neuronal nicotinic receptors: From structure to pathology. *Prog. Neurobiol.* **2004**, *74*, 363–396. [[CrossRef](#)] [[PubMed](#)]
8. Gotti, C.; Fornasari, D.; Clementi, F. Human neuronal nicotinic receptors. *Prog. Neurobiol.* **1997**, *53*, 199–237. [[CrossRef](#)]
9. Hogg, R.C.; Raggenbass, M.; Bertrand, D. Nicotinic acetylcholine receptors: From structure to brain function. In *Reviews of Physiology, Biochemistry and Pharmacology*; Springer: Berlin/Heidelberg, Germany, 2003; Volume 147, pp. 1–46.
10. Gotti, C.; Zoli, M.; Clementi, F. Brain nicotinic acetylcholine receptors: Native subtypes and their relevance. *Trends Pharmacol. Sci.* **2006**, *27*, 482–491. [[CrossRef](#)]
11. Oz, M.; Petroianu, G.; Lorke, D.E.  $\alpha$ 7-Nicotinic Acetylcholine Receptors: New Therapeutic Avenues in Alzheimer's Disease. In *Nicotinic Acetylcholine Receptor Technologies*; Li, M.D., Ed.; Neuromethods; Springer: New York, NY, USA, 2016; pp. 149–169, ISBN 978-1-4939-3768-4.
12. Nagele, R.G.; D'Andrea, M.R.; Anderson, W.J.; Wang, H.-Y. Intracellular accumulation of  $\beta$ -amyloid1–42 in neurons is facilitated by the  $\alpha$ 7 nicotinic acetylcholine receptor in Alzheimer's disease. *Neuroscience* **2002**, *110*, 199–211. [[CrossRef](#)]
13. Wang, H.Y.; Lee, D.H.; Davis, C.B.; Shank, R.P. Amyloid peptide A $\beta$ (1-42) binds selectively and with picomolar affinity to alpha7 nicotinic acetylcholine receptors. *J. Neurochem.* **2000**, *75*, 1155–1161. [[CrossRef](#)] [[PubMed](#)]
14. Bencherif, M.; Lippiello, P.M. Alpha7 neuronal nicotinic receptors: The missing link to understanding Alzheimer's etiopathology? *Med. Hypotheses* **2010**, *74*, 281–285. [[CrossRef](#)] [[PubMed](#)]
15. Prusiner, S.B. A Unifying Role for Prions in Neurodegenerative Diseases. *Science* **2012**, *336*, 1511–1513. [[CrossRef](#)] [[PubMed](#)]
16. Jucker, M.; Walker, L.C. Self-propagation of pathogenic protein aggregates in neurodegenerative diseases. *Nature* **2013**, *501*, 45. [[CrossRef](#)] [[PubMed](#)]
17. Meyer-Luehmann, M.; Coomaraswamy, J.; Bolmont, T.; Kaeser, S.; Schaefer, C.; Kilger, E.; Neuenschwander, A.; Abramowski, D.; Frey, P.; Jaton, A.L.; et al. Exogenous induction of cerebral beta-amyloidogenesis is governed by agent and host. *Science* **2006**, *313*, 1781–1784. [[CrossRef](#)] [[PubMed](#)]
18. Barykin, E.P.; Mitkevich, V.A.; Kozin, S.A.; Makarov, A.A. Amyloid  $\beta$  Modification: A Key to the Sporadic Alzheimer's Disease? *Front. Genet.* **2017**, *8*. [[CrossRef](#)] [[PubMed](#)]
19. Shimizu, T.; Watanabe, A.; Ogawara, M.; Mori, H.; Shirasawa, T. Isoaspartate formation and neurodegeneration in Alzheimer's disease. *Arch Biochem Biophys* **2000**, *381*, 225–234. [[CrossRef](#)]
20. Kozin, S.A.; Mitkevich, V.A.; Makarov, A.A. Amyloid- $\beta$  containing isoaspartate 7 as potential biomarker and drug target in Alzheimer's disease. *Mendeleev Commun.* **2016**, *26*, 269–275. [[CrossRef](#)]
21. Kozin, S.A.; Barykin, E.P.; Mitkevich, V.A.; Makarov, A.A. Anti-amyloid Therapy of Alzheimer's Disease: Current State and Prospects. *Biochem. Mosc.* **2018**, *83*, 1057–1067. [[CrossRef](#)]

22. Roher, A.E.; Lowenson, J.D.; Clarke, S.; Wolkow, C.; Wang, R.; Cotter, R.J.; Reardon, I.M.; Zürcher-Neely, H.A.; Heinrichson, R.L.; Ball, M.J. Structural alterations in the peptide backbone of beta-amyloid core protein may account for its deposition and stability in Alzheimer's disease. *J. Biol. Chem.* **1993**, *268*, 3072–3083.
23. Moro, M.L.; Phillips, A.S.; Gaimster, K.; Paul, C.; Mudher, A.; Nicoll, J.A.R.; Boche, D. Pyroglutamate and Isoaspartate modified Amyloid-Beta in ageing and Alzheimer's disease. *Acta Neuropathol. Commun.* **2018**, *6*. [[CrossRef](#)] [[PubMed](#)]
24. Kozin, S.A.; Cheglakov, I.B.; Ovsepyan, A.A.; Telegin, G.B.; Tsvetkov, P.O.; Lisitsa, A.V.; Makarov, A.A. Peripherally Applied Synthetic Peptide isoAsp7-A $\beta$ (1-42) Triggers Cerebral  $\beta$ -Amyloidosis. *Neurotox. Res.* **2013**, *24*, 370–376. [[CrossRef](#)] [[PubMed](#)]
25. Barykin, E.P.; Petrushanko, I.Y.; Kozin, S.A.; Telegin, G.B.; Chernov, A.S.; Lopina, O.D.; Radko, S.P.; Mitkevich, V.A.; Makarov, A.A. Phosphorylation of the Amyloid-Beta Peptide Inhibits Zinc-Dependent Aggregation, Prevents Na,K-ATPase Inhibition, and Reduces Cerebral Plaque Deposition. *Front. Mol. Neurosci.* **2018**, *11*. [[CrossRef](#)] [[PubMed](#)]
26. Gu, S.; Matta, J.A.; Lord, B.; Harrington, A.W.; Sutton, S.W.; Davini, W.B.; Brecht, D.S. Brain  $\alpha$ 7 Nicotinic Acetylcholine Receptor Assembly Requires NACHO. *Neuron* **2016**, *89*, 948–955. [[CrossRef](#)] [[PubMed](#)]
27. Tsetlin, V.I.; Hucho, F. Snake and snail toxins acting on nicotinic acetylcholine receptors: Fundamental aspects and medical applications. *FEBS Lett.* **2004**, *557*, 9–13. [[CrossRef](#)]
28. Encinas, M.; Iglesias, M.; Liu, Y.; Wang, H.; Muhaisen, A.; Ceña, V.; Gallego, C.; Comella, J.X. Sequential Treatment of SH-SY5Y Cells with Retinoic Acid and Brain-Derived Neurotrophic Factor Gives Rise to Fully Differentiated, Neurotrophic Factor-Dependent, Human Neuron-Like Cells. *J. Neurochem.* **2000**, *75*, 991–1003. [[CrossRef](#)] [[PubMed](#)]
29. Shelukhina, I.; Zhmak, M.; Lobanov, A.; Ivanov, I.; Garifulina, A.; Kravchenko, I.; Rasskazova, E.; Salmova, M.; Tukhovskaya, E.; Rykov, V.; et al. Azemiopsin, a Selective Peptide Antagonist of Muscle Nicotinic Acetylcholine Receptor: Preclinical Evaluation as a Local Muscle Relaxant. *Toxins* **2018**, *10*, 34. [[CrossRef](#)] [[PubMed](#)]
30. Shelukhina, I.; Spirova, E.; Kudryavtsev, D.; Ojomoko, L.; Werner, M.; Methfessel, C.; Hollmann, M.; Tsetlin, V. Calcium imaging with genetically encoded sensor Case12: Facile analysis of  $\alpha$ 7/ $\alpha$ 9 nAChR mutants. *PLoS ONE* **2017**, *12*, e0181936. [[CrossRef](#)] [[PubMed](#)]
31. Sitzia, F.; Brown, J.T.; Randall, A.; Dunlop, J. Voltage- and Temperature-Dependent Allosteric Modulation of  $\alpha$ 7 Nicotinic Receptors by PNU120596. *Front. Pharmacol.* **2011**, *2*. [[CrossRef](#)] [[PubMed](#)]
32. Hajós, M.; Hurst, R.S.; Hoffmann, W.E.; Krause, M.; Wall, T.M.; Higdon, N.R.; Groppi, V.E. The Selective  $\alpha$ 7 Nicotinic Acetylcholine Receptor Agonist PNU-282987 [N-[(3R)-1-Azabicyclo[2.2.2]oct-3-yl]-4-chlorobenzamide Hydrochloride] Enhances GABAergic Synaptic Activity in Brain Slices and Restores Auditory Gating Deficits in Anesthetized Rats. *J. Pharmacol. Exp. Ther.* **2005**, *312*, 1213–1222. [[CrossRef](#)] [[PubMed](#)]
33. Adzhubei, A.A.; Anashkina, A.A.; Makarov, A.A. Left-handed polyproline-II helix revisited: Proteins causing proteopathies. *J. Biomol. Struct. Dyn.* **2017**, *35*, 2701–2713. [[CrossRef](#)] [[PubMed](#)]
34. Jayaram, B.; Bhushan, K.; Shenoy, S.R.; Narang, P.; Bose, S.; Agrawal, P.; Sahu, D.; Pandey, V. Bhageerath: An energy based web enabled computer software suite for limiting the search space of tertiary structures of small globular proteins. *Nucleic Acids Res.* **2006**, *34*, 6195–6204. [[CrossRef](#)] [[PubMed](#)]
35. Phillips, J.C.; Braun, R.; Wang, W.; Gumbart, J.; Tajkhorshid, E.; Villa, E.; Chipot, C.; Skeel, R.D.; Kalé, L.; Schulten, K. Scalable molecular dynamics with NAMD. *J. Comput. Chem.* **2005**, *26*, 1781–1802. [[CrossRef](#)] [[PubMed](#)]
36. Anashkina, A.A.; Kravatsky, Y.; Kuznetsov, E.; Makarov, A.A.; Adzhubei, A.A. Meta-server for automatic analysis, scoring and ranking of docking models. *Bioinformatics* **2018**, *34*, 297–299. [[CrossRef](#)] [[PubMed](#)]
37. Guan, Z.-Z.; Yu, W.-F.; Shan, K.-R.; Nordman, T.; Olsson, J.; Nordberg, A. Loss of nicotinic receptors induced by beta-amyloid peptides in PC12 cells: Possible mechanism involving lipid peroxidation. *J. Neurosci. Res.* **2003**, *71*, 397–406. [[CrossRef](#)] [[PubMed](#)]
38. Inestrosa, N.C.; Godoy, J.A.; Vargas, J.Y.; Arrazola, M.S.; Rios, J.A.; Carvajal, F.J.; Serrano, F.G.; Farias, G.G. Nicotine Prevents Synaptic Impairment Induced by Amyloid- $\beta$  Oligomers Through  $\alpha$ 7-Nicotinic Acetylcholine Receptor Activation. *NeuroMolecular Med.* **2013**, *15*, 549–569. [[CrossRef](#)] [[PubMed](#)]
39. Bitan, G. Structural Study of Metastable Amyloidogenic Protein Oligomers by Photo-Induced Cross-Linking of Unmodified Proteins. In *Methods in Enzymology; Amyloid, Prions, and Other Protein Aggregates, Part C*; Academic Press: Cambridge, MA, USA, 2006; Volume 413, pp. 217–236.

40. Corradi, J.; Bouzat, C. Understanding the Bases of Function and Modulation of  $\alpha 7$  Nicotinic Receptors: Implications for Drug Discovery. *Mol. Pharmacol.* **2016**, *90*, 288–299. [[CrossRef](#)]
41. Spurny, R.; Debaveye, S.; Farinha, A.; Veys, K.; Vos, A.M.; Gossas, T.; Atack, J.; Bertrand, S.; Bertrand, D.; Danielson, U.H.; et al. Molecular blueprint of allosteric binding sites in a homologue of the agonist-binding domain of the  $\alpha 7$  nicotinic acetylcholine receptor. *Proc. Natl. Acad. Sci.* **2015**, *112*, E2543–E2552. [[CrossRef](#)]
42. Gay, E.A.; Giniatullin, R.; Skorinkin, A.; Yakel, J.L. Aromatic residues at position 55 of rat  $\alpha 7$  nicotinic acetylcholine receptors are critical for maintaining rapid desensitization. *J. Physiol.* **2008**, *586*, 1105–1115. [[CrossRef](#)]
43. Magdesian, M.H.; Nery, A.A.; Martins, A.H.B.; Juliano, M.A.; Juliano, L.; Ulrich, H.; Ferreira, S.T. Peptide blockers of the inhibition of neuronal nicotinic acetylcholine receptors by amyloid beta. *J. Biol. Chem.* **2005**, *280*, 31085–31090. [[CrossRef](#)]
44. Birks, J.S. Cholinesterase inhibitors for Alzheimer's disease. *Cochrane Database Syst. Rev.* **2006**. [[CrossRef](#)]
45. Nordberg, A. Nicotinic receptor abnormalities of Alzheimer's disease: Therapeutic implications. *Biol. Psychiatry* **2001**, *49*, 200–210. [[CrossRef](#)]
46. Liu, Q.; Kawai, H.; Berg, D.K. beta -Amyloid peptide blocks the response of alpha 7-containing nicotinic receptors on hippocampal neurons. *Proc. Natl. Acad. Sci. USA* **2001**, *98*, 4734–4739. [[CrossRef](#)] [[PubMed](#)]
47. Mitkevich, V.A.; Petrushanko, I.Y.; Yegorov, Y.E.; Simonenko, O.V.; Vishnyakova, K.S.; Kulikova, A.A.; Tsvetkov, P.O.; Makarov, A.A.; Kozin, S.A. Isomerization of Asp7 leads to increased toxic effect of amyloid-beta42 on human neuronal cells. *Cell Death Dis* **2013**, *4*, e939. [[CrossRef](#)] [[PubMed](#)]
48. Lyukmanova, E.N.; Shulepko, M.A.; Kudryavtsev, D.; Bychkov, M.L.; Kulbatskii, D.S.; Kasheverov, I.E.; Astapova, M.V.; Feofanov, A.V.; Thomsen, M.S.; Mikkelsen, J.D.; et al. Human Secreted Ly-6/uPAR Related Protein-1 (SLURP-1) Is a Selective Allosteric Antagonist of  $\alpha 7$  Nicotinic Acetylcholine Receptor. *PLoS ONE* **2016**, *11*, e0149733. [[CrossRef](#)] [[PubMed](#)]
49. Peng, X.; Katz, M.; Gerzanich, V.; Anand, R.; Lindstrom, J. Human alpha 7 acetylcholine receptor: cloning of the alpha 7 subunit from the SH-SY5Y cell line and determination of pharmacological properties of native receptors and functional alpha 7 homomers expressed in *Xenopus* oocytes. *Mol. Pharmacol.* **1994**, *45*, 546–554. [[PubMed](#)]
50. Zheng, X.; Xie, Z.; Zhu, Z.; Liu, Z.; Wang, Y.; Wei, L.; Yang, H.; Yang, H.; Liu, Y.; Bi, J. Methyllycaconitine Alleviates Amyloid- $\beta$  Peptides-Induced Cytotoxicity in SH-SY5Y Cells. *PLoS ONE* **2014**, *9*, e111536. [[CrossRef](#)] [[PubMed](#)]
51. Spirova, E.N.; Ivanov, I.A.; Kasheverov, I.E.; Kudryavtsev, D.S.; Shelukhina, I.V.; Garifulina, A.I.; Son, L.V.; Lummis, S.C.R.; Malca-Garcia, G.R.; Bussmann, R.W.; et al. Curare alkaloids from Matis Dart Poison: Comparison with d-tubocurarine in interactions with nicotinic, 5-HT<sub>3</sub> serotonin and GABA<sub>A</sub> receptors. *PLoS ONE* **2019**, *14*, e0210182. [[CrossRef](#)]
52. Manetti, D.; Garifulina, A.; Bartolucci, G.; Bazzicalupi, C.; Bellucci, C.; Chiamonte, N.; Dei, S.; Di Cesare Mannelli, L.; Ghelardini, C.; Gratteri, P.; et al. New Rigid Nicotine Analogues, Carrying a Norbornane Moiety, Are Potent Agonists of  $\alpha 7$  and  $\alpha 3^*$  Nicotinic Receptors. *J. Med. Chem.* **2019**, *62*, 1887–1901. [[CrossRef](#)]
53. Kryukova, E.V.; Ivanov, I.A.; Lebedev, D.S.; Spirova, E.N.; Egorova, N.S.; Zouridakis, M.; Kasheverov, I.E.; Tzartos, S.J.; Tsetlin, V.I. Orthosteric and/or Allosteric Binding of  $\alpha$ -Conotoxins to Nicotinic Acetylcholine Receptors and Their Models. *Mar. Drugs* **2018**, *16*. [[CrossRef](#)]
54. Durek, T.; Shelukhina, I.V.; Tae, H.-S.; Thongyoo, P.; Spirova, E.N.; Kudryavtsev, D.S.; Kasheverov, I.E.; Faure, G.; Corringer, P.-J.; Craik, D.J.; et al. Interaction of Synthetic Human SLURP-1 with the Nicotinic Acetylcholine Receptors. *Sci. Rep.* **2017**, *7*, 16606. [[CrossRef](#)] [[PubMed](#)]
55. Williams, D.K.; Wang, J.; Papke, R.L. Investigation of the molecular mechanism of the  $\alpha 7$  nicotinic acetylcholine receptor positive allosteric modulator PNU-120596 provides evidence for two distinct desensitized states. *Mol. Pharmacol.* **2011**, *80*, 1013–1032. [[CrossRef](#)] [[PubMed](#)]
56. Hurst, R.S.; Hajós, M.; Raggenbass, M.; Wall, T.M.; Higdon, N.R.; Lawson, J.A.; Rutherford-Root, K.L.; Berkenpas, M.B.; Hoffmann, W.E.; Piotrowski, D.W.; et al. A novel positive allosteric modulator of the alpha7 neuronal nicotinic acetylcholine receptor: In vitro and in vivo characterization. *J. Neurosci. Off. J. Soc. Neurosci.* **2005**, *25*, 4396–4405. [[CrossRef](#)] [[PubMed](#)]
57. Grønlien, J.H.; Håkerud, M.; Ween, H.; Thorin-Hagene, K.; Briggs, C.A.; Gopalakrishnan, M.; Malysz, J. Distinct profiles of alpha7 nAChR positive allosteric modulation revealed by structurally diverse chemotypes. *Mol. Pharmacol.* **2007**, *72*, 715–724. [[CrossRef](#)] [[PubMed](#)]

58. Ospina, J.A.; Broide, R.S.; Acevedo, D.; Robertson, R.T.; Leslie, F.M. Calcium Regulation of Agonist Binding to  $\alpha 7$ -Type Nicotinic Acetylcholine Receptors in Adult and Fetal Rat Hippocampus. *J. Neurochem.* **1998**, *70*, 1061–1068. [[CrossRef](#)] [[PubMed](#)]
59. Khiroug, L.; Giniatullin, R.; Klein, R.C.; Fayuk, D.; Yakel, J.L. Functional Mapping and  $\text{Ca}^{2+}$  Regulation of Nicotinic Acetylcholine Receptor Channels in Rat Hippocampal CA1 Neurons. *J. Neurosci.* **2003**, *23*, 9024–9031. [[CrossRef](#)] [[PubMed](#)]
60. Liu, Q.-S.; Berg, D.K. Extracellular Calcium Regulates Responses of Both  $\alpha 3$ - and  $\alpha 7$ -Containing Nicotinic Receptors on Chick Ciliary Ganglion Neurons. *J. Neurophysiol.* **1999**, *82*, 1124–1132. [[CrossRef](#)] [[PubMed](#)]
61. Maatuk, N.; Samson, A.O. Modeling the binding mechanism of Alzheimer's  $\text{A}\beta 1\text{--}42$  to nicotinic acetylcholine receptors based on similarity with snake  $\alpha$ -neurotoxins. *NeuroToxicology* **2013**, *34*, 236–242. [[CrossRef](#)]
62. Lyukmanova, E.N.; Shenkarev, Z.O.; Shulepko, M.A.; Mineev, K.S.; D'Hoedt, D.; Kasheverov, I.E.; Filkin, S.Y.; Krivolapova, A.P.; Janickova, H.; Dolezal, V.; et al. NMR Structure and Action on Nicotinic Acetylcholine Receptors of Water-soluble Domain of Human LYNX1. *J. Biol. Chem.* **2011**, *286*, 10618–10627. [[CrossRef](#)]
63. D'Andrea, M.R.; Nagele, R.G. Targeting the alpha 7 nicotinic acetylcholine receptor to reduce amyloid accumulation in Alzheimer's disease pyramidal neurons. *Curr. Pharm. Des.* **2006**, *12*, 677–684. [[CrossRef](#)]
64. Nichols, W.A.; Henderson, B.J.; Yu, C.; Parker, R.L.; Richards, C.I.; Lester, H.A.; Miwa, J.M. Lynx1 Shifts  $\alpha 4\beta 2$  Nicotinic Receptor Subunit Stoichiometry by Affecting Assembly in the Endoplasmic Reticulum. *J. Biol. Chem.* **2014**, *289*, 31423–31432. [[CrossRef](#)] [[PubMed](#)]
65. George, A.A.; Bloy, A.; Miwa, J.M.; Lindstrom, J.M.; Lukas, R.J.; Whiteaker, P. Isoform-specific mechanisms of  $\alpha 3\beta 4^*$ -nicotinic acetylcholine receptor modulation by the prototoxin lynx1. *FASEB J.* **2017**, *31*, 1398–1420. [[CrossRef](#)] [[PubMed](#)]
66. Xue, M.; Zhu, L.; Zhang, J.; Qiu, J.; Du, G.; Qiao, Z.; Jin, G.; Gao, F.; Zhang, Q. Low Dose Nicotine Attenuates  $\text{A}\beta$  Neurotoxicity through Activation Early Growth Response Gene 1 Pathway. *PLoS ONE* **2015**, *10*, e0120267. [[CrossRef](#)] [[PubMed](#)]
67. Wang, H.Y.; Bakshi, K.; Shen, C.; Frankfurt, M.; Trocme-Thibierge, C.; Morain, P. S 24795 limits beta-amyloid-alpha7 nicotinic receptor interaction and reduces Alzheimer's disease-like pathologies. *Biol. Psychiatry* **2010**, *67*, 522–530. [[CrossRef](#)] [[PubMed](#)]
68. Messi, M.L.; Renganathan, M.; Grigorenko, E.; Delbono, O. Activation of  $\alpha 7$  nicotinic acetylcholine receptor promotes survival of spinal cord motoneurons. *FEBS Lett.* **1997**, *411*, 32–38. [[CrossRef](#)]
69. Dajas-Bailador, F.A.; Lima, P.A.; Wonnacott, S. The  $\alpha 7$  nicotinic acetylcholine receptor subtype mediates nicotine protection against NMDA excitotoxicity in primary hippocampal cultures through a  $\text{Ca}^{2+}$  dependent mechanism. *Neuropharmacology* **2000**, *39*, 2799–2807. [[CrossRef](#)]
70. Ren, K.; Puig, V.; Papke, R.L.; Itoh, Y.; Hughes, J.A.; Meyer, E.M. Multiple calcium channels and kinases mediate  $\alpha 7$  nicotinic receptor neuroprotection in PC12 cells. *J. Neurochem.* **2005**, *94*, 926–933. [[CrossRef](#)]
71. Barykin, E.P.; Petrushanko, I.Y.; Burnysheva, K.M.; Makarov, A.A.; Mitkevich, V.A. Isomerization of Asp7 increases the toxic effects of amyloid beta and its phosphorylated form in SH-SY5Y neuroblastoma cells. *Mol. Biol.* **2016**, *50*, 863–869.
72. Abramov, A.Y.; Canevari, L.; Duchen, M.R. Calcium signals induced by amyloid  $\beta$  peptide and their consequences in neurons and astrocytes in culture. *Biochim. Biophys. Acta* **2004**, *1742*, 81–87. [[CrossRef](#)]
73. Abramov, A.Y.; Canevari, L.; Duchen, M.R. Changes in Intracellular Calcium and Glutathione in Astrocytes as the Primary Mechanism of Amyloid Neurotoxicity. *J. Neurosci.* **2003**, *23*, 5088–5095. [[CrossRef](#)]
74. Demuro, A.; Parker, I.; Stutzmann, G.E. Calcium Signaling and Amyloid Toxicity in Alzheimer Disease. *J. Biol. Chem.* **2010**, *285*, 12463–12468. [[CrossRef](#)] [[PubMed](#)]

